Blunt Body Aerodynamics for Hypersonic Low Density Flows

James N. Moss*, Christopher E. Glass*, and Francis A. Greene*

*NASA Langley Research Center, MS 408A, Hampton, VA 23681-2199

Abstract. Numerical simulations are performed for the Apollo capsule from the hypersonic rarefied to the continuum regimes. The focus is on flow conditions similar to those experienced by the Apollo 6 Command Module during the high altitude portion of its reentry. The present focus is to highlight some of the current activities that serve as a precursor for computational tool assessments that will be used to support the development of aerodynamic data bases for future capsule flight environments, particularly those for the Crew Exploration Vehicle (CEV). Results for aerodynamic forces and moments are presented that demonstrate their sensitivity to rarefaction; that is, free molecular to continuum conditions. Also, aerodynamic data are presented that shows their sensitivity to a range of reentry velocities, encompassing conditions that include reentry from low Earth orbit, lunar return, and Mars return velocities (7.7 to 15 km/s). The rarefied results obtained with direct simulation Monte Carlo (DSMC) codes are anchored in the continuum regime with data from Navier-Stokes simulations.

INTRODUCTION

Blunt-body space capsules form much of the legacy of the international manned space programs. With NASA's recently announced Constellation Program for exploring the moon, Mars and beyond, once again a blunt-body configuration has been selected as the capsule for the Crew Exploration Vehicle (CEV). The CEV includes a capsule much like Apollo, but larger, and like Apollo will be attached to a service module for life support and propulsion. Mission applications of the CEV include that of a low-Earth-orbit (LEO) version with a crew of six to the International Space Station, a lunar version that would carry a crew of four, and a Mars version that would carry a crew of six.

With commitments to evolve the CEV design(s) for LEO, lunar, and Mars missions, aerothermodynamic data bases will be generated utilizing computational and experimental (both ground-based and flight) resources. These new data bases along with an extensive capsule heritage, particularly that from Apollo (Refs. [1–4], for example), will provide the basis for optimizing the CEV's design, with particular emphasis on safety, flexibility, and affordability. The current study expands on the results presented in Ref. [5] where the focus was on the aerodynamics of the Apollo Command Module during the transitional portion of its reentry, from free molecular to continuum conditions. New results included in the present study are solutions obtained with a different DSMC code [6] and comparisons of the numerical simulations with flight and ground-based measurements. The primary focus is on flow conditions similar to those experienced by the Apollo 6 flight test, with a reentry velocity of 9.6 km/s at -25° angle of attack. Numerical simulations for the transitional flow regime are made with the 3D DSMC codes of Bird [7] and LeBeau [6] and for the continuum regime with the 3D Navier-Stokes (NS) code of Gnoffo [8]. Results are presented that show the sensitivity of the capsule aerodynamics to a wide range of altitude or rarefaction conditions and the sensitivity of the aerodynamics to velocity and angle-of-attack variations at an altitude of 105 km. Also, results from the DSMC and NS simulations show that the calculated aerodynamics are reasonably consistent near the 95 km altitude conditions. Lessons learned from this study can be applied to simulating other capsule configurations, such as the proposed CEV.

NUMERICAL PROGRAMS AND MODEL PARAMETERS

DSMC Analyses

For the more rarefied flow conditions, two DSMC codes, DS3V and DAC (DSMC Analysis Code), were used to both generate the data and provide a check on the consistency of the results. The majority of these calculations were made with the DS3V program of Bird [7], a general 3D code that provides both time-accurate unsteady flow and time-averaged steady flow simulations. In the current study, a scalar version of this program was used and all the present simulations were made by using a 3.2 GHz personal computer with a memory of 2.0 GB. The DAC program of LeBeau [6] provides both scalar and parallel processing options. Parallel processing is accomplished by domain decomposition and the parallel version of DAC is employed in the current study. For both DSMC programs, the molecular collisions are simulated with the variable hard sphere molecular model. The Larsen-Borgnakke statistical model [9] controls the energy exchange between kinetic and internal modes. All simulations are performed by using a five-species reacting air gas model while considering energy exchange between translation, rotational, and vibrational modes. Also, the surface is assumed to be noncatalytic and at a specified wall temperature. As for gas-surface interactions, they are assumed to be diffuse, with full energy accommodation.

An indicator of the resolution achieved in a DS3V simulation is given by the ratio of the mean collision separation between collision partners to the local mean free path (*mcs/mfp*). As demonstrated in Ref. [5], the average value for this parameter over the computational domain should be approximately 0.1 or less to obtain grid resolved aerodynamics. The total number of simulated molecules used in the current DS3V simulations ranged from approximately 1 to 16 million, and the grid adaption produced nominally 20 simulated molecules per collision cell.

For the DAC code, the user can implement a sequence of grid refinements of the two-level Cartesian grid such that the cell size is small in relation to the local mean free path. The current DAC simulations used between 8 to 460 million molecules, depending on the altitude, with the cell dimension equal to or less than the local mean free path. Both DSMC codes used the same definition for the Apollo surface geometry; that is, an unstructured grid consisting of 1912 points and 3718 triangles while making use of the problem symmetry such that the flow is computed about only half of the vehicle. This surface resolution was deemed adequate after a calculation was made for a case with a much finer surface grid resoultion (5946 and 11,178 points and triangles, respectively) and with a negligible change in results.

Navier-Stokes Analyses

Navier-Stokes analyses are performed by using the LAURA computational fluid dynamics code [8]. LAURA is an upwind-bias, point- or line-implicit relaxation algorithm for obtaining the numerical solution to the Navier-Stokes equations for three-dimensional, viscous, hypersonic flows in thermochemical nonequilibrium. LAURA has both the thin layer and full NS options, and both options were exercised in the current study. All of the LAURA simulations assumed the flow to be a reacting gas mixture with the surface boundary conditions consisting of a constant wall temperature, a noncatalytic surface, and no slip or temperature jump. The volume grid consists of 24 blocks with a total of 1 966 000 cells, and in the direction normal to the wall, there are 80 cells, which cover the region from the wall to the outer boundary. Grid adaption assured that the cell Reynolds numbers adjacent to the wall were at a nominal value no greater than 0.5 for the highest altitude (95 km) and 5.0 for the lowest altitude (65 km). The structured surface grid consisted of 24 576 cells. To balance the computational load, calculations were performed on 12 dual processor 2.8 GHz Opteron workstations with one block assigned to each of the 24 processors. Solutions were considered converged when the surface properties became steady and changed little after additional integration cycles.

Free Molecular and Newtonian Analyses

The free molecular (FM) and modified Newtonian (MN) results were obtained with the DACFREE code of R. G. Wilmoth (private communication, July 2005). DACFREE computes aerodynamic forces and moments on arbitrary bodies using standard free molecular and modified Newtonian methods. This code can handle arbitrary geometries specified as an unstructured collection of triangles, and for the present study, the surface grid was the same as that used in the DSMC simulations.

CONDITIONS AND RESULTS

Conditions

Considerable resources were devoted to quantifying the impact of the aerothermodynamic environment on the Apollo Command Module during reentry, particularly the thermal protection system. Reference [1] lists some of the reentry parameters for the 4 unmanned Apollo heat-shield-qualification flight tests, two at orbital entry velocities and two at superorbital entry velocities. The current study focuses on an altitude range from 200 to 65 km at 9.6 km/s (corresponding to the Apollo 6 reentry condition) and -25° angle of attack, for a range of incidence angles at an altitude of 105 km, and for a range of reentry velocities (7.68 to 15 km/s) at 105 km altitude.

The axisymmetric geometry for the Apollo Command Module used in the present study is shown in Fig. 1. The Apollo capsule was flown at an angle of attack while using an offset center of gravity (cg), where the cg coordinates used in the current study are listed in Fig. 1.

When the pressures and shear stresses are integrated over the surface, the resultant force acts at the capsule center-of-pressure (cp). The total force vector can be resolved into components, and the nomenclature used for the body (axial, C_A, and normal, C_N) and velocity (drag, C_D, and lift, C_L) oriented coordinates are as shown in Fig. 2.

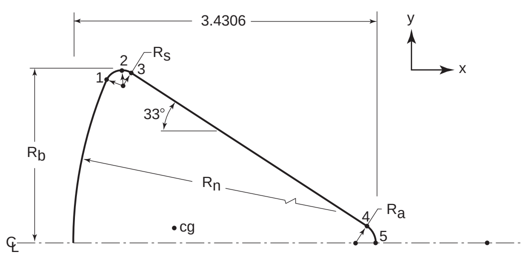

Location	x	y	s
1	0.3743	1.8368	1.8872
2	0.5543	1.9558	2.1158
3	0.6608	1.9242	2.2284
4	3.3254	0.1938	5.4056
5	3.3406	0.0000	5.6355
cg	1.1455	0.1600	-

D_b = 3.9116
R_b = 1.9558
R_n = 4.6939
R_s = 0.1956
R_a = 0.2311

Dimensions in m

Fig. 1. Apollo outer mold line.

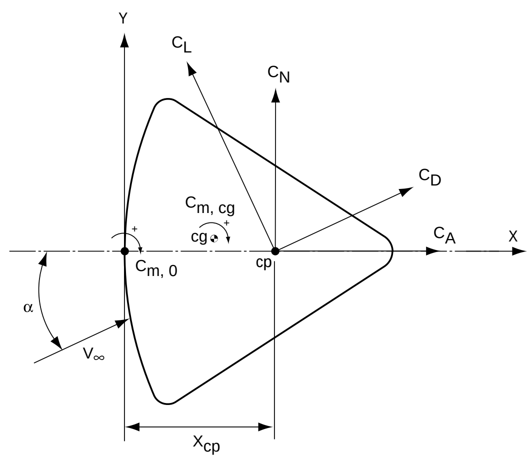

Fig. 2. Nomenclature for aerodynamic forces.

Free-stream atmospheric conditions (details given in Ref. [5]) are based on the data of Jacchia [10] (an exospheric temperature of 1200 K) for altitudes of 90 km and above and on that of Ref. [11] for altitudes less than 90 km. The surface temperatures are assumed to be uniformly distributed at constant values based on stagnation point heating conditions as discussed in Ref. [5]. The free-stream Knudsen numbers listed in the figures are based on the free-stream number density, a characteristic length of 3.912 m (maximum capsule diameter), and a constant molecular diameter of 3.78 x 10^{-10} m.

Effects of Rarefaction

Results presented in Fig. 3 provide an overall summary of the Apollo aerodynamics as obtained with the DSMC and NS programs. Results are presented in terms of a hard sphere free-stream Knudsen number with a coverage of approximately six orders of magnitude. As shown previously [12] for a related blunt body configuration, the pressure contribution is fairly constant, but the shear contribution increases with altitude such that the drag coefficient increases and the lift coefficient decreases. As detailed in Ref. [5], the DS3V results included in this figure are those that are grid resolved to an accuracy of probably 3 percent or better. Examination of the grid sensitivity results [5] provide qualitative information as to the effect of grid resolution on simulated aerodynamics; that is, poor volume grid resolution for the Apollo capsule resulted in an over prediction of the drag, axial, and normal force coefficients and an under prediction of the lift and lift-to-drag coefficients.

Sensitivity studies conducted with the NS calculations [5] indicated that the aerodynamics were insensitive to ionization effects; that is, the use of a 5-species neutral gas model as used in all the DSMC simulations or one that accounted for neutrals, ions, and electrons with a 11-species gas model did not signifficantly affect the results. Furthermore, it was shown that the NS results were insensitive to whether the thin-layer or full NS equations were used at the lower altitude conditions (85 km), but other studies [13] have shown that the full NS solutions provide higher fidelity results for the more rarefied conditions.

Also included in Fig. 3 are the new DAC results that provide grid resolved solutions to an altitude of 95 km, overlapping the NS results. Differences in the two DSMC sets of solutions are larger than expected, and currently it is not known what they might be attributed to. Perhaps they are because of simulation or physical model differences, or possibly user implementation. Specifically, differences in the two simulations for common altitudes between 110 to 100 km are less than 4 percent for drag, lift, axial, and moment (about the nose) coefficients, but 7 percent for L/D and as much as 12 percent for the normal force coefficient. However, the DSMC and NS results (overlap for DAC and extrapolated for DS3V) show generally consistent agreement in the vicinity of 95 km, or a hard sphere Knudsen number of 0.014. Note that rarefaction effects are present at 95 km and lower altitudes; however, the integrated effect on the aerodynamics is apparently not that significant.

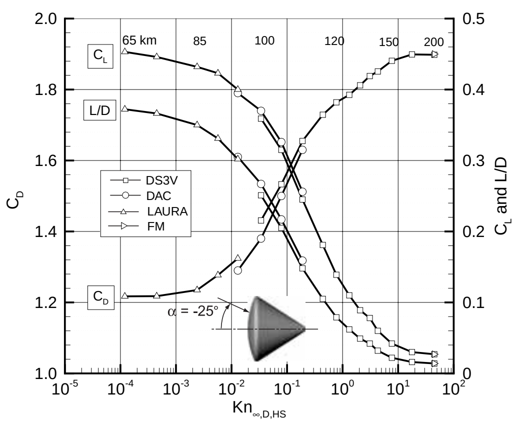

Fig. 3a. Drag, lift and L/D coefficients.

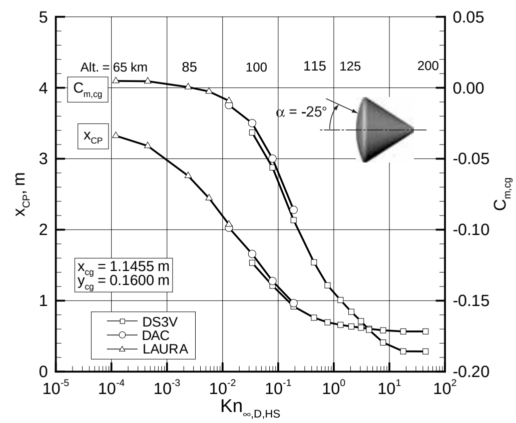

Fig. 3b. Center of pressure and moment coefficients.

FIGURE 3. Effect of rarefaction on aerodynamics as calculated with DSMC and NS codes.

Figure 3b details the movement of the center of pressure and the corresponding moment coefficient about the center of gravity as a function of Knudsen number. As the capsule descends from 200 to 65 km, the center of pressure experiences a substantial translation as it moves from a position forward of the center of gravity to one well aft. The corresponding change in the moment coefficient is from a negative value to a small positive value.

Effects of Angle of Attack

Figure 4 presents results of the DS3V simulations that show the dependence of the Apollo capsule aerodynamics to variations in angle of attack at 105 km altitude conditions and 9.6 km/s. Figure 4a highlights the dependence of L/D on incidence angle and also demonstrates its sensitivity to rarefaction by including the free molecular (FM) and modified Newtonian (MN) results. The FM and MN results were generated with the DACFREE code at the 200 km and 85 km conditions (free-stream gas composition changes with altitude), respectively.

Results for the center of pressure location and the moment coefficient about the offset center of gravity are presented in Fig. 4b. These simulations show that the stable trim point for the Apollo capsule at 105 km altitude occurs at an incidence angle of -164 degrees rather than the nominal -25 degrees flown by Apollo 6; that is, the capsule is statically unstable for much, if not all, of the transitional flow regime, a result not that uncommon for capsules in the transitional rarefied regime.

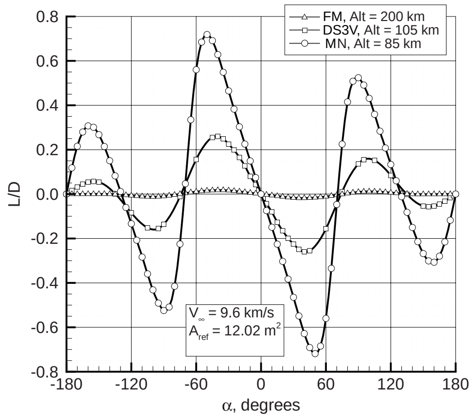

Fig. 4a. L/D coefficients.

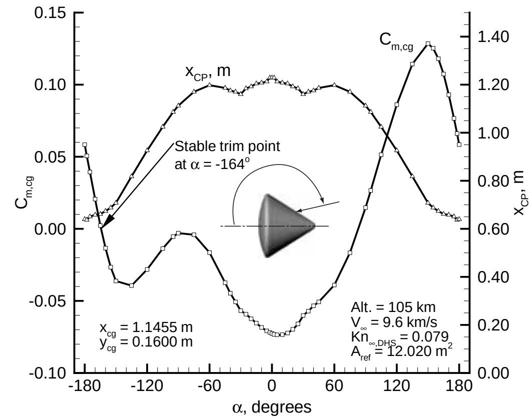

Fig. 4b. Center of pressure and moment coefficients.

FIGURE 4. Effect of angle of attack on aerodynamics as calculated with DS3V and DACFREE codes.

Effects of Free-Stream Velocity

To examine the effects of free-stream velocity variations, DS3V simulations were made for the Apollo capsule at an altitude of 105 km and -25 degrees incidence for 5 free-stream velocities ranging from 7.7 to 15 km/s. Four of the velocities correspond to the nominal re-entry conditions of the 4 unmanned Apollo qualification flight tests [1]. The 15 km/s velocity is representative of the upper bounds for a Mars return mission. Consequently, this range of entry velocities is inclusive of that for reentry from LEO, lunar return, and Mars return missions. Results of the simulations for variations in free-stream velocity show (Fig. 5) that the changes in the aerodynamic coefficients with increasing velocity are similar to those incurred with increasing rarefaction; that is, the magnitude of the drag, axial, and normal force coefficients increases with increasing free-stream velocity while the magnitude of the lift and lift-to-drag ratio coefficients decreases with increasing velocity. These findings are consistent with the correlations demonstrated by Wilhite et al. [14] (Fig. 7, p 172) for the Shuttle Orbiter axial-force coefficients as a function of a viscous correlation parameter.

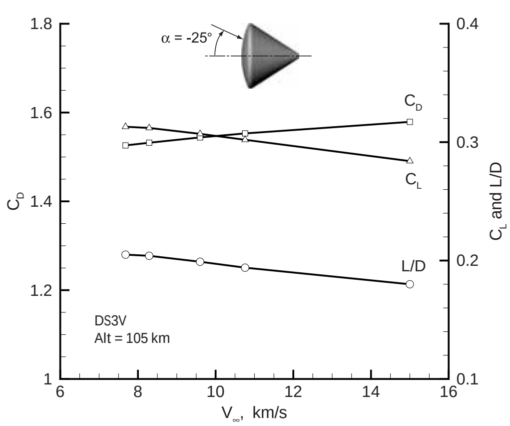

Fig. 5. Effect of velocity on aerodynamics.

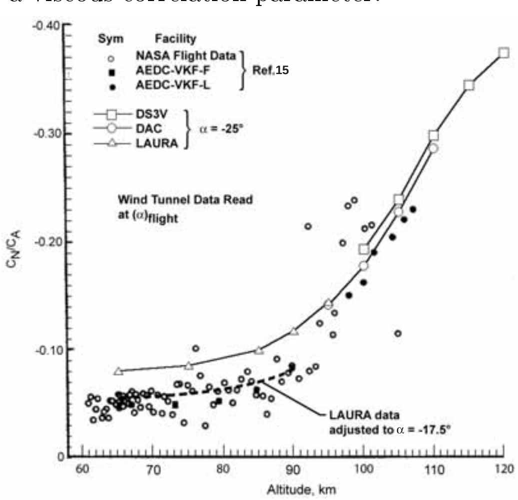

Fig. 6. Flight, computed, and wind tunnel data.

Comparison with Flight and Wind Tunnel Data

Figure 6 presents the results of the present calculations for the aerodynamic ratio of normal-to-axial force coefficients as a function of altitude. Also included in this figure are the flight data for the (Apollo-Saturn) AS-202 unmanned flight test (relative entry velocity of 8.29 km/s) and wind tunnel measurements made at the Arnold Engineering Development Center (AEDC) [15]. As indicated in Fig. 7a of Ref. [15], the angle of attack for most of the AS-202 reentry was less than the -25° experienced by the Apollo 6 mission. The flight inferred [4] angles of attack for AS-202 were near -25° for altitudes of 110 to 100 km, and then decreased to approximately -17.5° at 92 km and remained near this value as the capsule descended through 60 km. When the NS results for the Apollo 6 mission are adjusted to account for the AS-202 flight attitude, then good agreement between flight and computation is obtained. An approximate adjustment is made based on the DS3V results at the 105 km altitude condition in which a reduction in angle of attack from -25° to -17.5° produces a 31 percent reduction in the value of C_N/C_A. When this correction factor is applied to the 4 calculated values at altitudes below 92 km, the results are displayed by the dashed line in Fig. 6, with generally good agreement between flight and calculated results for two sets of conditions: 110 to 100 km at -25° and 92 to 60 km at -17.5°.

CONCLUSIONS

Significant findings of the present investigation are: (1) the current numerical results are shown to be consistent with flight data for normal-to-axial force ratios, (2) the Apollo Command Module is statically unstable for much of the rarefied flow regime, (3) changes in the aerodynamic coefficients with increasing velocity have the same trend as that for increasing rarefaction, (4) the DSMC simulations are shown to be reasonably consistent based on the results from two different codes, and (5) close agreement in aerodynamics is obtained with DSMC and NS programs for the 95 km altitude condition; thereby, providing a capability for calculating hypersonic blunt body aerodynamics for the spectrum of flows that include free molecular, transitional, and continuum conditions without relying on bridging functions.

REFERENCES

1. Lee, D. B., "Apollo Experience Report–Aerothermodynamics Evaluation," NASA TN D-6843, June 1972.
2. Lee, D. B. and Goodrich, W. D., "The Aerothermodynamic Environment of the Apollo Command Module During Superorbital Entry," NASA TN D-6792, April 1972.
3. Lee, D. B., Bertin, J. J., and Goodrich, W. D., "Heat-Transfer Rate and Pressure Measurements Obtained During Apollo Orbital Entries," NASA TN D-6028, April 1970.
4. Hillje, E. R., "Entry Flight Aerodynamics from Apollo Mission AS-202," NASA TN D-4185, October 1967.
5. Moss, J. N., Glass, C. G., and Greene, F. A., "DSMC Simulations of Apollo Capsule Aerodynamics for Hypersonic Rarefied Conditions," AIAA Paper 2006-3577, June 2006.
6. LeBeau, G. J., "A Parallel Implementation of the Direct Simulation Monte Carlo Method," *Computer Methods in Applied Mechanics and Engineering, Parallel Computational Methods for Flow Simulation and Modeling*, Vol. 174, 1999, pp. 319-337.
7. Bird, G. A., *Visual DSMC Program for Three-Dimensional Flows.* The DS3V Program User's Guide, Version 1.2, March 2005.
8. Cheatwood, F. M., and Gnoffo, P. A., "User's Manual for the Langley Aerothermodynamic Upwind Relaxation Algorithm (LAURA)," NASA TM 4674, April 1996.
9. Borgnakke, C., and Larsen, P. S., "Statistical Collision Model for Monte Carlo Simulation of Polyatomic Gas Mixture," *Journal of Computational Physics*, Vol. 18, No. 4, 1975, pp. 405-420.
10. Jacchia, L. G., "Thermospheric Temperature, Density, and Composition: New Models," Smithsonian Astrophysical Observatory, Cambridge, MA, Special Rept. 375, March 1977.
11. Anon, "U. S. Standard Atmosphere, 1962," Dec. 1962.
12. Celenligil, M. C., Moss, J. N., and Blanchard, R. C., "Three-Dimensional Rarefied Flow Simulations for the Aeroassist Flight Experiment Vehicle," *AIAA Journal*, Vol. 29, No.1, 1991, pp. 52-57.
13. Moss, J. N., Glass, C. G., Hollis, B. R., and Van Norman, J. W., "Low-Density Aerothermodynamics of the Inflatable Re-entry Vehicle Experiment (IRVE)," AIAA Paper 2006-1189, Jan. 2006.
14. Wilhite, A. W., Arrington, J. P., and McCandless, R. S., "Performance Aerodynamics of Aeroassisted Orbital Transfer Vehicles," *Progress in Astronautics and Aeronautics*, Vol. 96, *Thermal Design of Aeroassisted Orbital Transfer Vehicles*, edited by H.F. Nelson, AIAA, New York, 1985, pp. 165-185.
15. Boylan, D. E. and Griffith, B. J. "Simulation of the Apollo Command Module Aerodynamics at Re-Entry Altitudes," *Proceedings of the Third National Conference on Aerospace Meteorology*, American Meteorological Society, Boston, May 6-9, 1968, pp. 370-378.